[Frontiers in Bioscience, Landmark, 20, 1036-1046, June 1, 2015]

Identification of biomarkers for bone union promoted by mechanical stimulation

Yanjie Guo[1], Shangchun Guo[1], Nanji Lu[1], Yimin Chai[1], Xingang Yu[1]

[1]Department of Orthopedic Surgery, Sixth People's Hospital, Shanghai Jiaotong University, Shanghai, China

TABLE OF CONTENTS

1. ABSTRACT

At present, the identity of the proteins that participate in mechanical stimulation during the fracture healing process is not known. Here, we screened for and identified 299 proteins that are expressed in various stages of mechanically stimulated fracture healing. Among these biomarkers, 54 proteins were differentially expressed during all three recovery time points. Gene ontology (GO) analysis and selected biomarker candidates were used to determine their involvement in biological processes required for mechanically stimulated healing. The levels of cofilin-1 and A2HSG protein were significantly upregulated in the forth week after fracture suggesting that that they play a role in mechanically stimulated fracture healing.

2. INTRODUCTION

It is well known that fracture repair is comprised of four stages: inflammation, soft callus formation, hard callus formation, and remodeling (1). The remodeling process during healing is fundamentally similar to normal bone maintenance and thus requires the absorption of bone by osteoclasts, tightly coupled deposition of new bone by osteocytes, and the formation of osteons (2). Although rigid immobilization is necessary for proper healing prior to the formation of a bony callus within the fracture gap, mechanical stimulation has also been shown to stimulate bone remodeling in the newly formed callus and thus improve the stiffness of newly formed bone (3). Increased stressing force and stress cycling frequency increases bone formation up to a point, beyond which no improvement is observed (2,4). In addition, excessive stability in an immobilized fracture can prolong the healing process and reduce bone density (5).

The transduction of mechanical stimuli to bone growth and healing requires three processes:

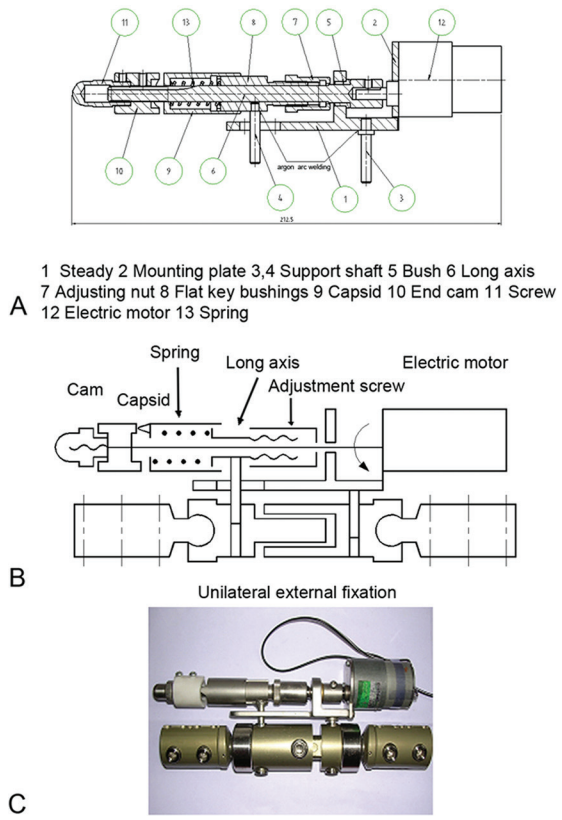

Figure 1. Schematic diagrams and photograph of the stress stimulation instrument. A. The internal structure of the cam-driving device. B. The operating principle of cam-driving device. C. A photograph of the external fixator.

the biochemical sensing of mechanical stimuli, signal transduction, and the effector-cell response (6). Some progress has been made in elucidating the mechanisms, proteins and pathways involved in this process. Osteocytes are well positioned in the bone to detect mechanical stress, and studies have demonstrated that these cells produce prostaglandins in response to a pulsing fluid flow (PFF) (7,8) caused by mechanical stimulation. Indeed, the pharmaceutical inhibition of prostaglandin production inhibits bone remodeling (9). PFF raises the intracellular Ca2+ concentration by activating pressure-sensitive ion channels in combination with the release of Ca2+ from intracellular stores in a Ca2+ and inositol trisphosphate-dependent manner. Ca2+ and protein kinase C then stimulate phospholipase A2 activity, arachidonic acid production, and ultimately prostaglandin E2 release (10). COX-2 is also induced in response to fluid shear in a C/EBP beta, AP-1, and CREB dependent manner (11).

Bone healing is a highly complex process involving a wide range of different cell types, and one would expect the involvement of a wide range of genes and proteins from a variety of different regulatory pathways. To further expand the list of proteins known to be involved in the bone remodeling response to mechanical stimuli and improve our understanding of the mechanism of bone healing, we developed a novel stress-induction instrument. The mechanical stimulation using this device promotes bone fracture healing in a sheep model of mid-shaft tibial osteotomy.

We then quantified protein expression in bony callus formed in the presence and absence of externally applied stress using the isobaric tags for relative and absolute quantitation (iTRAQ) method of peptide quantification in combination with nanoscale liquid chromatography coupled to tandem mass spectrometry (Nano LC−MS/MS).

3. MATERIALS AND METHODS

3.1. Instrument design

For this study, we designed an instrument that creates a dynamic mechanical load in a sheep model of tibial osteotomy for the promotion of bone union. The length of the dynamic loading device is 28 cm , and the width is 4 cm. The connecting rod is adjustable, which can be adjusted in the range of 7-12 cm. The main parts of the device includes cam, capsid spring, adjustment screw and the electric motor. The cam is made of high strength polyethylene .The capsid and spring is made of stainless steel, and the rest is made of titanium alloy. We developed an external fixator with precise control over the actuation frequency and amplitude. This instrument provided controllable, axial, reciprocating stress stimulation to the fracture location (Figure 1) when attached to an external fixation stent.

3.2. Animals and surgery

Tibias from 30 sheep were randomly selected for osteotomy. The osteotomy defect was 2 mm in size, and the tibias subjected to osteotomy were fixed externally. Sheep were randomly divided into 2 groups (n = 15), where group A received stress stimulation. Ten days after surgery, the actuation device was attached to the stent, and stimulation was performed at 1 Hz and 0.2.5. mm of axial reciprocating stress for 30 min/d. Four weeks after surgery, stress stimulation was ended. The control group B was bracket fixed, but received no stress stimulation.

After 2, 4, and 6 weeks, 5 animals from each group were sacrificed, and fixation brackets were removed. Four centimeters of tibia was removed from around the center of the fracture line and stored in liquid nitrogen.

3.3. Protein preparation

Callus tissue samples were washed with phosphate buffered saline (PBS) and crushed and ground in a mortar containing liquid nitrogen. The resulting powder was immediately suspended in lysis buffer (7 M

urea, 2 M thiourea, 65 mM DTT, and 0.1.%PMSF from Sigma-Aldrich, USA). After the solution was vigorously stirred for 30 min, cell debris and insoluble materials were removed by centrifugation at 16,000xg for 15 min. Protein concentrations were determined using a modified Bradford method. The supernatants were aliquoted and stored at -80°C for further use.

3.4. iTRAQ labeling

We performed iTRAQ labeling with an iTRAQ Reagent 4-Plex kit from Applied Biosystems (Foster City, CA) using the manufacturer's protocol. Experimental samples from two, four and six weeks of stimulation were labeled with iTRAQ labeling reagents 114, 118 and 121, respectively. Control samples from two, four and six weeks were labeled with reagents 113, 117 and 119, respectively.

One hundred microliters of pooled sample (n=3) for each group was reduced with tris-(2-carboxyethyl) phosphine and alkylated with methyl methanethiosulfonate (MMTS). Trypsin (mass spectrometry grade, Promega, Madison, WI) was used to digest samples overnight at 37°C at a 1:20 ratio (W/W) of trypsin to protein.

The different labeling reactions were combined to perform the appropriate comparisons. Oasis HLB cartridges (Waters, Milford, MA) were used to desalt the mixtures, which were then dried in a vacuum centrifuge (Concentrator Plus, Eppendorf, Germany) (12).

3.5. Strong cation exchange (SCX)

iTRAQ-labeling peptides were fractionated with SCX chromatography using a 20AD HPLC system (Shimadzu, Kyoto, Japan) and a polysulfoethyl column (2.1. mm*100 mm, 5 μm, 200 Å, The Nest Group, Southborough, MA) to eliminate interfering materials, including MMTS, TCEP, calcium chloride, SDS, excess iTRAQ reagents, and dissolution buffer. The peptide mixture was dissolved in 80 μL of Buffer A containing 10 mM KH2PO4 in 25% acetonitrile pH 3 (Fisher Scientific, Fair Lawn, NJ) and then loaded onto a column. We separated peptides using a gradient of 0−80% Buffer B (Buffer A with 350 mM KCl) using a flow rate of 200 μL/min for 60 min. We monitored the absorbance at 214 nm and collected 20 SCX fractions in all. Eluted fractions were desalted with C18 cartridges (UltraMicroSpin, The Nest Group, Southborough, MA), dried, and then reconstituted in 20 μL of 0.1.% FA for nanoLC−MS/MS analysis.

3.6. NanoLC−MS/MS analysis

The peptide mixture was separated with Nano HPLC (Eksigent Technologies) and a secondary RP analytical column (Eksigent, C18, 3 μm, 150 mm x 75 μm). Phase B (98% acetonitrile with 0.1.% formic acid) was used to elute peptides under the following gradient conditions: 5-35% phase B for 1-45 min, 35-80% phase B for 45-47 min and 80% phase B for 47-49 min. The total flow rate was maintained at 300 nL/min. We used an electrospray voltage of 2.3. kV at the inlet of the mass spectrometer.

The AB SCIEX TripleTOF™ 5600 System (Applied biosystems) was operated in data-dependent mode to switch automatically between MS and MS/MS acquisition. MS spectra were acquired across the mass range of 350–1250 m/z in high-resolution mode using a 250 ms accumulation time per spectrum. Tandem mass spectra were scanned from 50–1250 m/z in high-sensitivity mode with rolling collision energy. The 20 most intense precursors were selected for fragmentation per cycle with a dynamic exclusion time of 9 s.

3.7. Protein identification and quantitation

The complete iTRAQ experimental data set was searched against the Swiss-Prot protein database using ProteinPilot 4.5. software (Applied Biosystems, Grand Island, NY, USA). ProteinPilot software used the Paragon algorithm to perform protein identification and the Pro Group algorithm to determine the minimal set of confident protein identifications. The ProteinPilot search parameters were set with trypsin cleavage specificity and cys alkylation (MMTC) as fixed modifications, biological modification "ID focus" settings, and a protein minimum confidence score of 95% (detected protein threshold >95% (unused ProtScore > 1.3.)). Common modifications, substitutions, and cleavage events were built-in functions of the software. ProteinPilot software pooled data from all LC/MS runs for each iTRAQ experiment. For iTRAQ quantification, the ratios of iTRAQ reporter ion intensities in MS/MS spectra (m/z 115.1., 116.1., 117.1., 118.1., 119.1., and 121.1.) were used for the relative quantification of each peptide. The ratio for each protein was calculated as a weighted average value combining averages of the peptide quantifications for this protein from all fractions. The accuracy of each protein ratio was estimated from a calculated error factor (EF) in Protein Pilot and the P value to assess whether the protein was significantly differentially expressed. For the selection of differentially expressed proteins, we considered the following situation: (1) the protein had to contain at least two unique, high-scoring peptides; (2) the proteins had to have a P value <0.0.5.; and (3) the proteins identified by mass tag change ratio had to be ≤0.7.5. or ≥1.3.

3.8. Network mapping

To identify network associations for both cofilin-1 and A2HSG, a separate protein-protein interaction (PPI) photo was created for each protein using the String database (string-db.org) (13), different proteins (Uniprot ID) as input, and the default String database parameters.

3.9. Western blotting

Triplicate samples containing approximately 30 μg of protein were combined with 10 μL of SDS

reducing buffer and heated to 60°C for 15 min. Samples were then cooled and loaded onto a SDS polyacrylamide gel (4% (v/v) stacking gel and 12% (v/v) separating gel) using the Laemmli SDS-PAGE buffer system. Gels were electrophoresed at 80 V for 10 min and then 150 V for 60 min. Proteins were then transferred to a nitrocellulose membrane at 85 mA in a Mini Trans-Blot Cell (Bio-Rad) for 2 h. Membranes were blocked in blocking buffer (5% w/v skimmed milk in tris-buffered saline and 0.0.5.% v/v Tween), and then incubated with a 1 to 1000 dilution of rabbit polyclonal anti-AHSG antibody (Abcam, Cambridge, U.K.) in blocking buffer overnight at 4°C. Membranes were washed three times with tris-buffered saline with 0.0.5.% v/v tween (TBS-tween) buffer and then incubated with a 1:3500 dilution of anti-rabbit IgG conjugated with horseradish peroxidase (Dako, Glostrup, Denmark) in blocking buffer for 45 min at room temperature. Membranes were again washed three times with TBS-tween, and membrane-bound proteins were detected with ECL Plus western Blotting reagent and exposure to X-ray film (GE Healthcare, Amersham, U.K.)

3.10. Immunohistochemistry

Ten percent formalin was used to fix dissected tibia for 7 days. The samples were then decalcified in 10% formic acid, dehydrated with an ethanol (20–100%) and xylene series, and embedded in paraffin (Paraplast X-Tra). Sections were attached to slides, deparaffinized, hydrated with an inverted xylene and ethanol series, and incubated with a 1/500 dilution of one of two different rabbit polyclonal antibodies specific for either A2HSG or cofilin-1 (Abcam, Cambridge, U.K.) in 1.5.% serum in PBS. Slides were then washed, incubated with a 1:5000 dilution of biotinylated anti-rabbit antibody, and developed with 3,3′-diaminobenzidine tetrahydrochloride (Vector Laboratories). Hematoxylin was then used to counterstain the slides.

3.11. Statistical Analysis

Statistical analyses were performed with SPSS 19.0. software (SPSS, Chicago, IL). A Pearson X2 test or an X2 test with continuity correction and Fisher's exact test were used to compare qualitative variables. Quantitative variables were analyzed using a Student's t or Mann-Whitney test. Experimental data were presented as the mean of each condition plus the standard deviation, and P <0.0.5. was considered statistically significant. Receiver operating characteristic (ROC) curves were used to determine the diagnostic values of the markers.

4. RESULTS

4.1. Screening for differentially expressed proteins

We used quantitative iTRAQ labeling and Nano LC−MS/MS to compare proteins extracted from healing tibia with and without stress stimulation. In this analysis, 299 proteins from various stages of fracture healing had a mass tag change ratio of ≤0.7.5. and ≥1.3. and a P value <0.0.5. (Table 1) in the stress stimulation group relative to the control and were thus scored as differentially expressed. Among these were 261 differentially expressed proteins from 2 weeks after fracture, of which 186 were up- and 75 were down-regulated. One hundred seventy-seven differentially expressed proteins were identified 4 weeks after fracture, and 93 of these were up- and 84 were down-regulated. One hundred seventy-nine differentially expressed proteins were identified 6 weeks after fracture, of which 120 were up- and 59 were down-regulated. The false positive rate (FDR) was less than 0.0.1.

4.2. GO analysis of differentially expressed proteins

To understand their functions and related processes, the differentially expressed proteins identified with iTRAQ were subjected to gene ontology (GO) analysis (Figure 2). Of the 299 proteins, 265 were annotated into 47 groups, including 30 categories in the biology process namespace, 7 categories in the cell component namespace and 10 categories in the molecular function namespace. GO analysis identified 12 proteins associated with response to stress, 41 proteins associated with cellular metabolic processes, 51 proteins involved in metabolic processes, 50 proteins in the regulation of biological processes, 89 proteins associated with various organelle and cellular components, and 81 proteins associated with catalysis.

The "Response To Stress" group contains proteins involved in injury repair, including CTHL2, A2HSG, Hsp70, CH3L1, AQP1, bactinecin 11, catalase, monocyte differentiation antigen CD14, and glutathione peroxidase. The "Developmental Process" group contained osteopontin, a protein central to bone formation, and trichohyalin, a protein that strengthens hair follicles and other epithelial tissues.

4.3. Hierarchical cluster analysis of stress stimulation and control groups and upregulation of individual proteins

We developed hierarchical groupings of our expression data to reveal associations between the different gene classifications in our data set. As can be seen in Figure 3A, we found that differentially expressed proteins involved in the stress response primarily appeared at the fourth and sixth weeks after fracture, while proteins related to bone formation, such as ossification and cell-matrix adhesion, appeared primarily at the second and fourth weeks. Cell division-related proteins were enriched in the sixth week.

Differentially expressed proteins were up-regulated for different cell components in each period

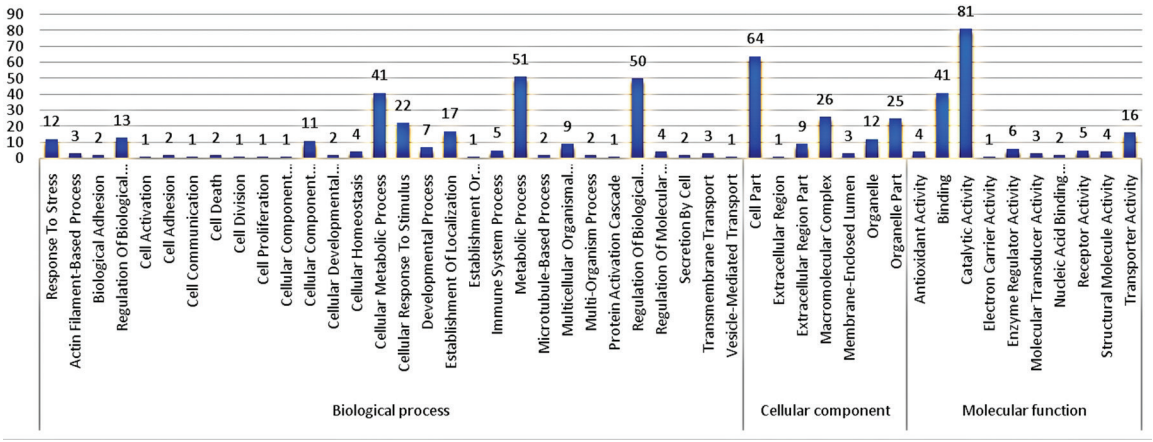

Figure 2. GO analysis of differentially expressed proteins. We subjected 299 differentially expressed proteins to GO analysis. Of these, 265 were successfully classified into 47 groups, including 30 categories in the biology process namespace, 7 categories in the cell component name space and 10 categories in the molecular function namespace.

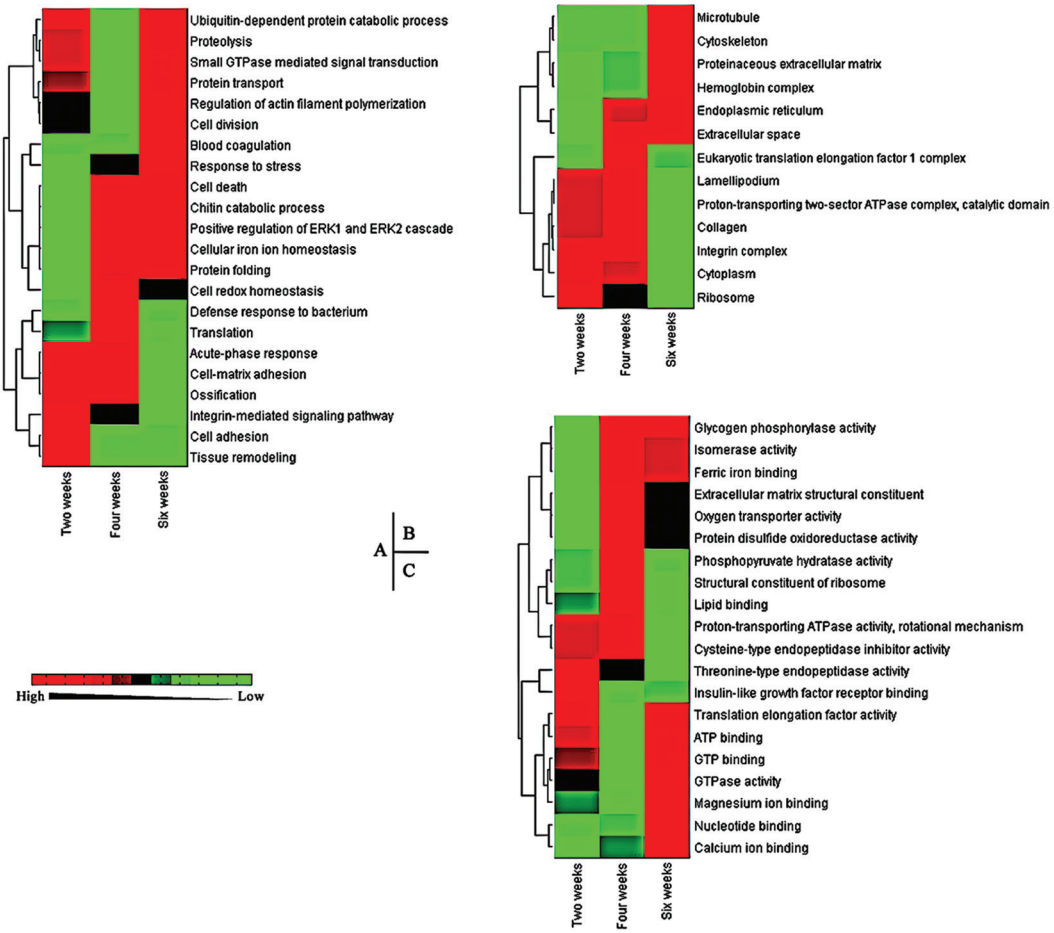

Figure 3. Hierarchical cluster analysis of the stress stimulation and control groups. Hierarchical cluster analysis of 265 proteins that were expressed with statistically significant differences (P < 0.0.1. and fold > 1.5.). A single column represents independent experiments from 2, 4, and 6 weeks after fracture from the stress-stimulation and control groups. The 3 main clusters of proteins are represented by either green-, black-, or red-colored bars. A hypergeometric distribution was used in enrichment analysis. A. Enrichment analysis of the biology process namespace. B. Enrichment analysis of the cell component namespace. C. Enrichment analysis of the molecular function namespace.

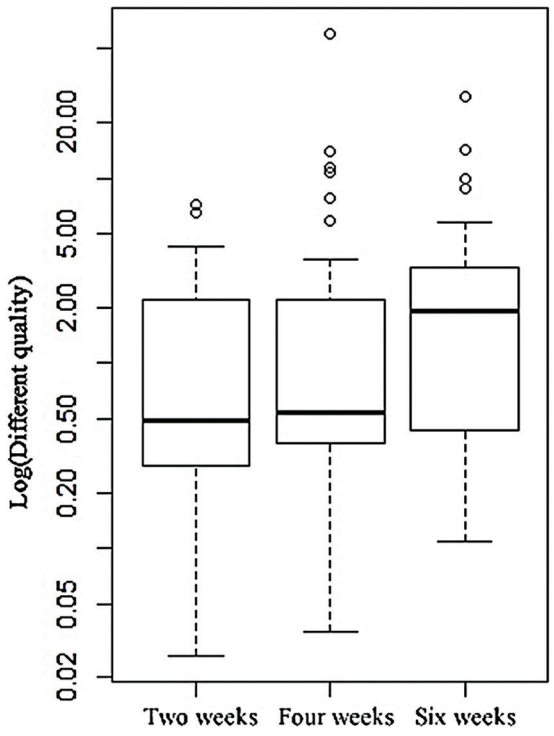

Figure 4. Comparison of differential expression levels for the 54 proteins that were differentially expressed in all three recovery time points (2, 4, and 6 weeks after fracture).

after fracture. Ribosomal protein levels were elevated at week two, eukaryotic translation elongation factor 1 complex was enriched at week four and microtubule, cytoskeletal, and extracellular matrix component levels were elevated at week six (Figure 3B).

There were also differences in protein function for the differentially expressed proteins in each period after fracture. For example, various ion- and nucleotide-binding activities were up-regulated at six weeks, while oxygen transporter activity, among others, was upregulated at week four (Figure 3C).

Table 2 catalogs the 54 individual proteins that were differentially expressed at all three recovery time points. Mass change ratios ranged from 0.1.2.5. to 7.1.7.8. at two weeks, 0.0.3.6. to 13.9.3.2. at four weeks, and 0.1.1.0. to 27.7.9.7. at six weeks. Overall, the up-regulation of these 54 differentially expressed proteins at six weeks after fracture was significantly higher than at weeks two and four ($P < 0.0.5.$; Figure 4).

4.4. Network analysis for the differentially expressed proteins cofilin-1 and A2HSG

The differentially expressed protein cofilin-1 and A2HSG were chose for further validation because neither protein has been directly implicated in bone healing. Cofilin-1 has been implicated in cytoskeleton function (16), while A2HSG has been associated with various aspects of bone metabolism (28,29). To identify direct and indirect protein associations for both cofilin-1 and A2HSG, separate protein-protein interaction (PPI) photos were created using the String database (string-db.org) using different proteins (Uniprot ID) (14) as input. Figure 5A depicts the resulting associations for cofilin-1 (CFL1), with strong interactions identified for LIMK1 and SHH1, suppressors and activators, respectively, of cofilin-1 (15), and also for LIMK2 and ACTA1, the primary targets of cofilin-1 activity (16). Interactions identified for A2HSG are shown in Figure 5B and include SERPINC1, APOA1 and 2, AMBP, and ALB.

4.5. Validation of differentially expressed proteins with western blotting

In Nano LC−MS/MS quantification, Cofilin-1 produced mass charge ratios of 1.2.6., 1.6.0., and 2.8.3. at 2, 4, and 6 weeks, respectively, following fracture, while A2HSG produced ratios of 0.1.6., 11.4., and 10.0. for 2, 4, and 6 weeks, respectively, and was thus dramatically overexpressed (data not shown). MS/MS spectra from Cofilin-1 and A2HSG are presented in Figures 6A and 6B, respectively. The amino acid sequences of matched peptides are also shown.

To verify the expression levels of these two proteins determined with Nano LC−MS/MS, we performed western blotting on three biological replicates from both the control and stress-treatment groups. B-actin was chosen as the expression and sample-loading control. Expression of cofilin-1 became elevated after four weeks post-fracture, and remained elevated at 6 weeks, with A2HSG following a similar pattern (Figure 7). Western blotting results were thus in rough agreement with iTRAQ data for both proteins.

4.6. Upregulation of Cofilin-1 and A2HSG at 4 weeks in the stress treatment group as revealed by histology and immunohistochemistry

The extent and location of Cofilin-1 and A2HSG protein expression in healing bone tissues in the presence and absence of mechanical stimulation was evaluated using immunohistochemical staining of bone tissue sections (Figure 8). Nuclear staining for Cofilin-1 was clearly visible in both control and experimental tissues at both two and four weeks post fracture. However, significant staining in bone matrix materials became apparent at four weeks post fracture. Although little nuclear staining was visible for A2HSG in either group or time period, faint staining occurred in the matrix for the control treatment at 4 weeks, while more substantial staining occurred in response to mechanical stimulation, also at week 4. These results agree with the protein expression data revealed with western blotting.

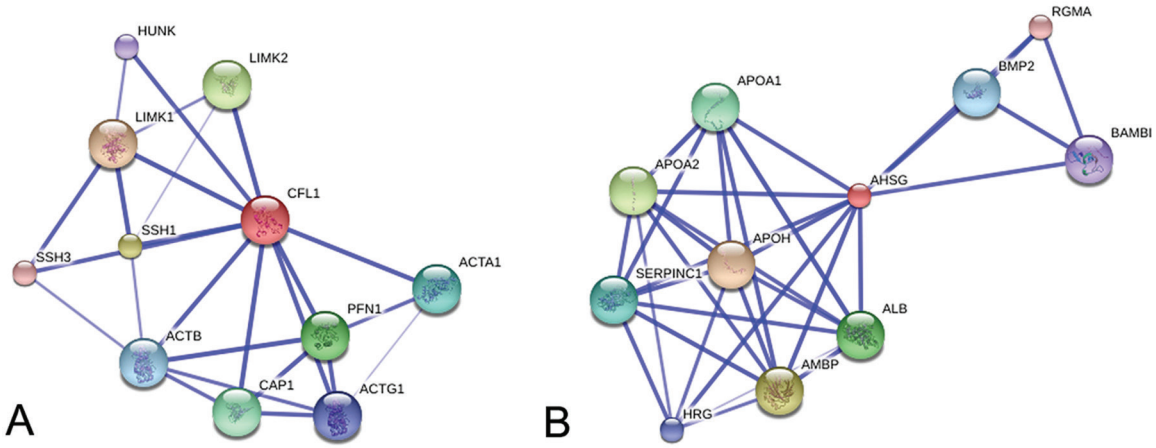

Figure 5. Protein−protein interactions determined by network analysis for the differentially expressed proteins cofilin-1 (A.) and A2HSG (B.). Interactions with high connectivity are indicated with strong lines.

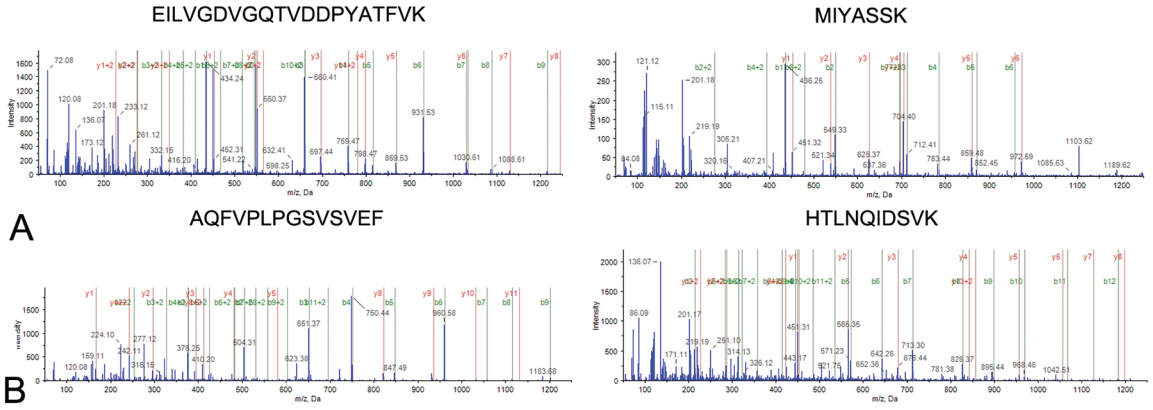

Figure 6. Representative MS/MS spectrum showing the peptides derived from cofilin-1 and A2HSG. A. MS/MS spectra showing the identified peptide sequences (EILVGDVGQTVDDPYATFVK and MIYASSK) that led to the identification of cofilin-1. B. The MS/MS spectra show the identified peptide sequences (AQFVPLPGSVSVEF and HTLNQIDSVK) that led to the identification of A2HSG.

5. DISCUSSION

The purpose of this study was to identify new proteins involved in the response of fracture healing to mechanical stimulation using the iTRAQ peptide quantification method and Nano LC−MS/MS. To meet this goal, we developed a new device for stress stimulation in a sheep model of midshaft tibial osteotomy that created a dynamic mechanical load to promote bone union using well-characterized physical parameters.

We identified 299 differentially expressed genes in our iTRAQ analysis. Many of these genes were involved in the response to stress, cellular metabolism, regulation, various organelle and cellular components, and catalysis.

First, the “Response To Stress” group contains a variety of proteins of interest in bone healing, including CTHL2, the 70 kD heat shock protein (Hsp70), CH3L1, aquaporin 1 (AQP1), bactinecin 11, catalase, monocyte differentiation antigen CD14, and glutathione peroxidase. These proteins are involved in the maintenance of organismal homeostasis in the face of external assaults.

These proteins contribute to bone healing in a variety of ways. CTHL2 and Bactinecin 11 are precursors of defense peptides produced in neutrophils (17) that are active in innate immunity, and Hsp70 is a part of the ubiquitin-proteasome system and thus participates in the ubiquitination and resulting degradation of misfolded proteins (18). Notably, researchers have demonstrated that Hsp70 may serve as a prognostic marker for surgery involving bone (19) because expression of this protein in bone tissue tracks with the severity of induced stress. AQP1 has been shown to promote the migration of bone marrow mesenchymal cells to fracture gaps and thus contributes to the regulation bone healing (20). Various studies have shown that reactive oxygen species (ROS)

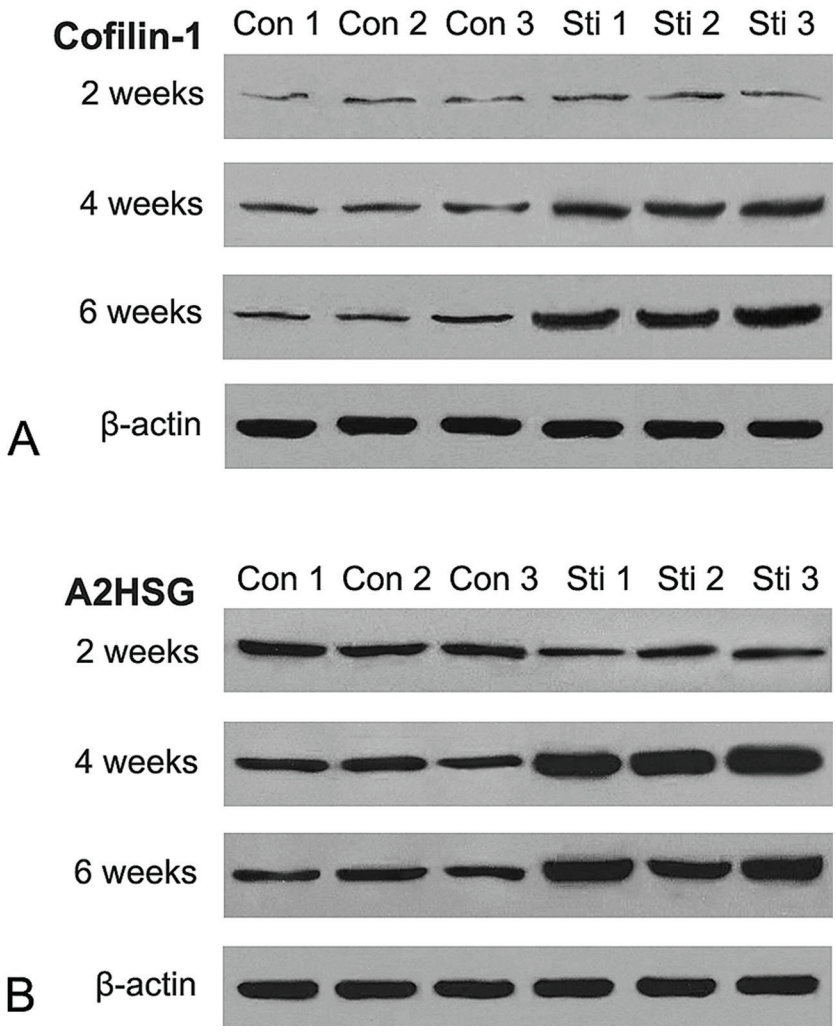

Figure 7. Western blot validation of differentially expressed proteins extracted from callus derived from the stress stimulation and control groups. A. Expression levels of Cofilin-1 (A.) and A2HSG (B.) at 2, 4 and 6 weeks post fracture, as indicated by representative western blots. "Con" indicates the control group and "Sti" indicates mechanical stimulation. β-Actin was used as the loading control for both proteins.

promote osteoclast formation and thus promote bone resorption (21,22). Elevation of catalase and glutathione peroxidase expression, which remove H2O2 from the cell, would likely inhibit the stimulation of bone resorption caused by H2O2 (23).

Proteins of interest were also found in the "Developmental Process" group. The protein osteopontin is expressed by a wide variety of cell types, including osteoclasts, osteoblasts, epithelial cells, chondrocytes, smooth muscle cells, macrophages and T cells, and osteopontin may promote cell adhesion and chemotaxis in bone resorption. Osteoclasts express osteopontin in their basolateral, clear zone, and ruffled border membranes. They also secrete the protein into the resorption pit (24) during bone resorption and remodeling, and thus osteopontin is found embedded in the cement lines of bone (25).

Trichohyalin was also placed in the "Developmental Process" group. This protein is thought to strengthen epithelial tissues such as the hair follicle inner root sheath (26). It has not been previously associated with bone structure and metabolism. Further investigation would help elucidate the role that this protein plays in bone healing.

Our study identified a wide variety of proteins that are known to be involved in the metabolism of bone, reinforcing the validity of our study design. Therefore, the presence of two proteins that had not previously been associated with the response of bone healing to mechanical stimulation attracted our attention. Cofilin-1 is well known to transduce signals from various regulatory pathways, such as the RhoA/Rho-associated kinase (ROCK) pathway, to actin (27) as was verified in our network analysis. Therefore, cofilin-1

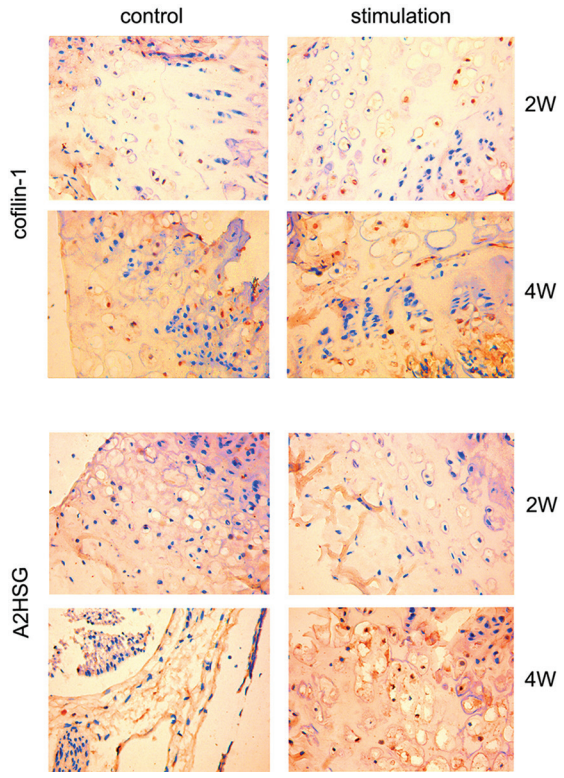

Figure 8. Immunohistochemistry of union bone samples from the stress stimulation and control groups. Tissues were probed with one of two different primary rabbit polyclonal antibodies specific for either A2HSG or cofilin-1. Brown staining indicates antibody binding, and tissues were counterstained with hematoxylin. 2W and 4W indicate two and four weeks, respectively.

plays a central role in cellular homeostasis due the importance of actin in a host of cellular functions such as muscle contraction, cell division, cellular mobility, and the maintenance of cellular morphology (16). Many different cell types, including osteocytes, osteoblasts, bone marrow mesenchymal cells, and various immune system cells among others must migrate into the fracture gap and the surrounding tissues to initiate bone healing, and the elevated expression of this protein during bone healing speaks to the importance of cell motility to this process.

A2HSG is a major serum protein that also incorporated into bone. This protein has been implicated in osteogenesis, bone resorption (28), and the inhibition of unneeded mineralization (29). Elevated serum levels of A2HSG have also been associated with osteogenesis imperfect (30). Mechanical stimulation dramatically increased the concentration of this protein in the hard callus, suggesting that investigations into the mechanism of A2HSG incorporation could lead to a significant improvement in our understanding of bone healing.

In conclusion, we used the iTRAQ peptide quantification method and Nano LC−MS/MS to find proteins that were differentially expressed in either the presence or absence of externally applied mechanical stimulation in a sheep model of midshaft tibial osteotomy. This analysis produced a list of 299 proteins that were differentially expressed spread across the three time points of 2, 4, and 6 weeks. Proteins annotated in the “stress response” group by GO analysis primarily appeared at the fourth and sixth weeks after fracture. Proteins related to bone formation, such as ossification and cell-matrix adhesion, appeared primarily at the second and fourth weeks. Overall, more proteins were differentially expressed at six weeks, and 54 proteins were differentially expressed at all three recovery time points. Of the differentially expressed proteins identified, we used western blotting and immunohistochemistry to verify that cofilin-1 and A2HSG protein-expression levels were significantly upregulated by the fourth week after fracture. These results indicated that cofilin-1 and A2HSG might play a role in mechanical stimulation during the fracture healing process. Overall, these results reinforced our current understanding of bone healing and provided new leads for further investigations into this process.

6. ACKNOWLEDGMENTS

This study was supported by Natural Science Foundation of China, Grant No.81101459, Funding agencies had no role in study design, data collection, analysis,decision to publish, or preparation of the manuscript.

7. REFERENCES

1. Schindeler A, McDonald MM, Bokko P, Little DG. Bone remodeling during fracture repair: The cellular picture. Semin. *Cell Dev Biol* 19(5), 459-66 (2008)
DOI: 10.1016/j.semcdb.2008.07.004
2. Robling AG, Castillo AB, Turner CH. Biomechanical and Molecular Regulation of Bone Remodeling. *Annu Rev Biomed Eng* 8(1), 455-98 (2006)
DOI: 10.1146/annurev.bioeng.8.061505.095721
3. Goodship AE, Kenwright J. The influence of induced micromovement upon the healing of experimental tibial fractures. *J Bone Joint Surg Br* 67-B(4), 650–5 (1985)
Doi not found.
4. Hsieh Y-F, Turner CH. Effects of Loading Frequency on Mechanically Induced Bone Formation. *J Bone Miner Res* 16(5), 918-24 (2001)
DOI: 10.1359/jbmr.2001.16.5.918
5. Frost HM. A 2003 Update of Bone Physiology

and Wolff's Law for Clinicians. *Angle Orthod* 74(1):3-15 (2004)
Doi not found.

6. Morgan EF, Gleason RE, Hayward LNM, Leong PL, Salisbury Palomares KT. Mechanotransduction and Fracture Repair. *J Bone Joint Surg Am* 90(Suppl 1), 25-30 (2008)
DOI: 10.2106/JBJS.G.01164

7. Ajubi NE, Klein-Nulend J, Nijweide PJ, Vrijheid-Lammers T, Alblas MJ, Burger EH. Pulsating Fluid Flow Increases Prostaglandin Production by Cultured Chicken Osteocytes-A Cytoskeleton-Dependent Process. *Biochem Biophys Res Commun* 225(1), 62-8 (1996)
DOI: 10.1006/bbrc.1996.1131

8. Klein-Nulend J, Burger EH, Semeins CM, Raisz LG, Pilbeam CC. Pulsating Fluid Flow Stimulates Prostaglandin Release and Inducible Prostaglandin G/H Synthase mRNA Expression in Primary Mouse Bone Cells. *J Bone Miner Res* 12(1), 45-51 (1997)
DOI: 10.1359/jbmr.1997.12.1.45

9. Pead MJ, Lanyon LE. Indomethacin modulation of load-related stimulation of new bone formation *in vivo*.Calcif. *Tissue Int* 45(1), 34-40 (1989)
DOI: 10.1007/BF02556658

10. Ajubi NE, Klein-Nulend J, Alblas MJ, Burger EH, Nijweide PJ. Signal transduction pathways involved in fluid flow-induced PGE2 production by cultured osteocytes. *Am J Physiol Endocrinol Metab* 276(1), E171-E178 (1999)
Doi not found.

11. Ogasawara A, Arakawa T, Kaneda T, Takuma T, Sato T, Kaneko H, Kumegawa M, Hakeda Y. Fluid Shear Stress-induced Cyclooxygenase-2 Expression Is Mediated by C/EBP β, cAMP-response Element-binding Protein, and AP-1 in Osteoblastic MC3T3-E1 Cells. *J Biol Chem* 276(10), 7048-54 (2001)
DOI: 10.1074/jbc.M008070200

12. Lin H, Zhang F, Geng Q, Yu T, Cui Y, Liu X, Li J, Yan M, Liu L, He X, Li J, Yao M. Quantitative Proteomic Analysis Identifies CPNE3 as a Novel Metastasis-promoting Gene in NSCLC. *J Proteome Res* 12(7), 3423-33 (2013)
DOI: 10.1021/pr400273z

13. Franceschini A, Szklarczyk D, Frankild S, Kuhn M, Simonovic M, Roth A, Lin J, Minguez P, Bork P, von Mering C, Jensen LJ. STRING v9.1.: protein-protein interaction networks, with increased coverage and integration. *Nucleic Acids Res* 41(D1), D808-D815 (2013)
DOI: 10.1093/nar/gks1094

14. Jin G-Z, Li Y, Cong W-M, Yu H, Dong H, Shu H, Liu X-H, Yan G-Q, Zhang L, Zhang Y, Kang X-N, Guo K, Wang Z-D, Yang P-Y, Liu Y-K. iTRAQ–2DLC–ESI–MS/MS Based Identification of a New Set of Immunohistochemical Biomarkers for Classification of Dysplastic Nodules and Small Hepatocellular Carcinoma. *J Proteome Res* 10(8), 3418-28 (2011)
DOI: 10.1021/pr200482t

15. Goyal P, Pandey D, Brunnert D, Hammer E, Zygmunt M, Siess W. Cofilin Oligomer Formation Occurs *In vivo* and Is Regulated by Cofilin Phosphorylation. *PLoS One* 8(8), e71769 (2013)
DOI: 10.1371/journal.pone.0071769

16. Bernstein BW, Bamburg JR. ADF/Cofilin: a functional node in cell biology. *Trends Cell Biol* 20(4), 187-95 (2010)
DOI: 10.1016/j.tcb.2010.01.001

17. Scocchi M, Bontempo D, Boscolo S, Tomasinsig L, Giulotto E, Zanetti M. Novel cathelicidins in horse leukocytes. *FEBS Lett* 457(3), 459-64 (1999)
DOI: 10.1016/S0014-5793(99)01097-2

18. McClellan AJ, Frydman J. Molecular chaperones and the art of recognizing a lost cause. *Nat Cell Biol* 3(2), E51-E53 (2001)
DOI: 10.1038/35055162

19. Gülnahar Y, HüseyinKöşger H, Tutar Y. A comparison of piezosurgery and conventional surgery by heat shock protein 70 expression. *Int J Oral Maxillofac Surg* 42(4), 508-10 (2013)
DOI: 10.1016/j.ijom.2012.10.027

20. Meng F, Rui Y, Xu L, Wan C, Jiang X, Li G. Aqp1 enhances migration of bone marrow mesenchymal stem cells through regulation of FAK and β-catenin. *Stem Cells Dev* 23(1), 66-75 (2014)
DOI: 10.1089/scd.2013.0185

21. Garrett IR, Boyce BF, Oreffo RO, Bonewald L, Poser J, Mundy GR. Oxygen-derived free radicals stimulate osteoclastic bone resorption in rodent bone *in vitro* and *in vivo*. *J Clin Invest* 85(3), 632-9 (1990)
DOI: 10.1172/JCI114485

22. Wauquier F, Leotoing L, Coxam V, Guicheux J, Wittrant Y. Oxidative stress in bone remodelling and disease. *Trends Mol Med* 15(10), 468-77 (2009)
DOI: 10.1016/j.molmed.2009.08.004

23. Lean JM, Jagger CJ, Kirstein B, Fuller K, Chambers TJ. Hydrogen Peroxide Is Essential for Estrogen-Deficiency Bone Loss and Osteoclast Formation. *Endocrinology* 146(2), 728-35 (2005)
DOI: 10.1210/en.2004-1021

24. Chellaiah MA, Kizer N, Biswas R, Alvarez U, Strauss-Schoenberger J, Rifas L, Rittling SR, Denhardt DT, Hruska KA. Osteopontin Deficiency Produces Osteoclast Dysfunction Due to Reduced CD44 Surface Expression. *Mol Biol Cell* 14(1), 173-89 (2003)
DOI: 10.1091/mbc.E02-06-0354

25. Dodds RA, Connor JR, James IE, Lee Rykaczewski E, Appelbaum E, Dul E, Gowen M. Human osteoclasts, not osteoblasts, deposit osteopontin onto resorption surfaces: An *in vitro* and *ex vivo* study of remodeling bone. *J Bone Miner Res* 10(11), 1666-80 (1995)
DOI: 10.1002/jbmr.5650101109

26. Steinert PM, Parry DAD, Marekov LN. Trichohyalin mechanically strengthens the hair follicle multiple cross-bridging roles in the inner root sheath. *J Biol Chem* 278(42), 41409-19 (2003)
DOI: 10.1074/jbc.M302037200

27. Fazal F, Bijli KM, Minhajuddin M, Rein T, Finkelstein JN, Rahman A. Essential Role of Cofilin-1 in Regulating Thrombin-induced RelA/p65 Nuclear Translocation and Intercellular Adhesion Molecule 1 (ICAM-1) Expression in Endothelial Cells. *J Biol Chem* 284(31), 21047-56 (2009)
DOI: 10.1074/jbc.M109.016444

28. Szweras M, Liu D, Partridge EA, Pawling J, Sukhu B, Clokie C, Jahnen-Dechent W, Tenenbaum HC, Swallow CJ, Grynpas MD, Dennis JW. α2-HS Glycoprotein/Fetuin, a Transforming Growth Factor-β/Bone Morphogenetic Protein Antagonist, Regulates Postnatal Bone Growth and Remodeling. *J Biol Chem* 277(22), 19991-7 (2002)
DOI: 10.1074/jbc.M112234200

29. Heiss A, DuChesne A, Denecke B, Grötzinger J, Yamamoto K, Renné T, Jahnen-Dechent W. Structural Basis of Calcification Inhibition by α2-HS Glycoprotein/Fetuin-A formation of colloidal calciprotein particles. *J Biol Chem* 278(15), 13333-41 (2003)
DOI: 10.1074/jbc.M210868200

30. Dickson IR, Bagga M, Paterson CR. Variations in the serum concentration and urine excretion of alpha 2HS-glycoprotein, a bone-related protein, in normal individuals and in patients with osteogenesis imperfecta. *Calcif Tissue Int* 35(1), 16-20 (1983)
DOI: 10.1007/BF02405000

31. Saroha A, Kumar S, Chatterjee BP, Das HR. Jacalin Bound Plasma O-Glycoproteome and Reduced Sialylation of Alpha 2-HS Glycoprotein (A2HSG) in Rheumatoid Arthritis Patients. *PLoS One* 7(10), e46374 (2012)
DOI: 10.1371/journal.pone.0046374

Abbreviations: iTRAQ: Isobaric tags for relative and absolute quantitation; NanoLC−MS/MS: nanoscale liquid chromatography coupled to tandem mass spectrometry;FDR: false positive rate;GO: gene ontology;PBS: phosphate buffered saline;PPI: protein-protein interaction;ROC: Receiver operating characteristic;

Key Words: iTRAQ, Mechanical Stimulation, Fracture Healing

Send correspondence to: Xingang Yu, Department of Orthopedic Surgery, Sixth People's Hospital, Shanghai Jiaotong University, No.600 Yishan Road, Shanghai200233, China, Tel: 18930172207, Fax:86-021-64369181, E-mail: yuxg1979@yeah.net